

# Growth responses to climate in a multi-species tree-ring network in the Western Carpathian Tatra Mountains, Poland and Slovakia

ULF BÜNTGEN,<sup>1,2</sup> DAVID C. FRANK,<sup>1</sup> RYSZARD J. KACZKA,<sup>3</sup> ANNE VERSTEGE,<sup>1</sup>  
TOMASZ ZWIJACZ-KOZICA<sup>4</sup> and JAN ESPER<sup>1</sup>

<sup>1</sup> Swiss Federal Research Institute WSL, Zürcherstrasse 111, 8903 Birmensdorf, Switzerland

<sup>2</sup> Corresponding author (buentgen@wsl.ch)

<sup>3</sup> Faculty of Earth Science, University of Silesia, 60 Bedzinska 50, 41–200 Sosnowiec, Poland

<sup>4</sup> Tatra National Park, Chalubinskiego 42a, 34–500 Zakopane, Poland

Received March 17, 2006; accepted June 6, 2006; published online February 1, 2007

**Summary** We analyzed growth responses to climate of 24 tree-ring width and four maximum latewood density chronologies from the greater Tatra region in Poland and Slovakia. This network comprises 1183 ring-width and 153 density measurement series from four conifer species (*Picea abies* (L.) Karst., *Larix decidua* Mill., *Abies alba* (L.) Karst., and *Pinus mugo* (L.)) between 800 and 1550 m a.s.l. Individual spline detrending was used to retain annual to multi-decadal scale climate information in the data. Twentieth century temperature and precipitation data from 16 grid-boxes covering the 48–50°N and 19–21°E region were used for comparison. The network was analyzed to assess growth responses to climate as a function of species, elevation, parameter, frequency and site ecology. Twenty ring-width chronologies significantly correlated ( $P < 0.05$ ) with June–July temperatures, whereas the latewood density chronologies were correlated with the April–September temperatures. Climatic effects of the previous-year summer generally did not significantly influence ring formation, whereas site elevation and frequency of growth variations (i.e., inter-annual and decadal) were significant variables in explaining growth response to climate. Response to precipitation increased with decreasing elevation. Correlations between summer temperatures and annual growth rates were lower for *Larix decidua* than for *Picea abies*. Principal component analysis identified five dominant eigenvectors that express somewhat contrasting climatic signals. The first principal component contained highest loadings from 11 *Picea abies* ring-width chronologies and one *Pinus mugo* ring-width chronology and explained 42% of the network's variance. The mean of these 12 high-elevation chronologies was significantly correlated at 0.62 with June–July temperatures, whereas the mean of three latewood density chronologies, which loaded most strongly on the fourth principal component, significantly correlated at 0.69 with April–September temperatures ( $P < 0.001$  over the 1901–2002 period in both cases). These groupings allow for a robust estimation of June–July (1661–2004) and April–September (1709–2004) temperatures, respec-

tively. Comparison with reconstructions from the Alps and Central Europe supports the general rule of the dominant influence of growing season temperature on high-elevation forest growth.

**Keywords:** climate change, dendrochronology, maximum latewood density, ring width.

## Introduction

Tree growth responses to climatic change are key to assessing future forest productivity, vegetation dynamics, plant diversity and species richness (e.g., Kienast et al. 1998, Saxe et al. 2001, Sitch et al. 2003, Thuiller et al. 2005), and to evaluating tree-ring-based temperature reconstructions (Briffa et al. 1998, Büntgen et al. 2006a). Although physiological studies provide empirical evidence on how trees react to internal (biotic) and external (abiotic) forcing agents (Kozłowski and Pallardy 1997), physiological studies of the longer-term responses of trees suffer from either the short-term nature of laboratory and field experiments with low spatial coverage, or the limited range of assessments of plant growth when larger regions are considered. An alternative approach is to study tree-ring width (TRW) and maximum latewood density (MXD) measurements which provide information on past growth rates. Radial growth of trees from higher elevations generally reflects temperature variations, whereas radial growth of trees from lower elevations generally mirrors precipitation changes (Schweingruber 1996). However, because of the co-variation of various climatic parameters and complex plant physiological reactions and processes (Tranquillini 1964), attempts to define growth responses in terms of a single controlling factor often fail (Fritts 1976). For example, eco-physiological studies in elevational ecotone sites where growth is predominantly limited by low summer temperatures emphasized the importance of various winter climate conditions (e.g., frost, desiccation, solar irradiance, freeze-thaw cy-

cles, soil frost and snow cover) on the vigor of woody plants (Vaganov et al. 1999, Oberhuber 2004). Local geographical settings including slope, aspect, wind-exposure and soil conditions provide second-order variations to the general rules of thermally constrained forest productivity at high altitudes and toward northern timberlines (Körner 1998), and water-limited constraints on forest productivity at mid- and low altitudes and latitudes (Leuzinger et al. 2005).

Analyses of the climatic influence on variations in European tree growth, from annual extremes to multi-decadal scale fluctuations, have mainly focused on high-elevation conifers from the Alpine arc (e.g., Rolland et al. 1998, Desplanque et al. 1999, Rolland et al. 2000, Carrer and Urbinati 2004, Neuwirth et al. 2004, Oberhuber 2004, Jolly et al. 2005). Analyses of large networks that include MXD measurements have examined growth response patterns to climatic conditions across the Alps (Frank and Esper 2005a) and Europe (Briffa et al. 2002). For the Carpathian arc, however, there have been no long-term dendroclimatological network analyses and only a few local studies have assessed the climatic influence on tree growth (Bednarz 1984, Feliksik 1993, Szychowska-Krapiec 1998, Bednarz et al. 1999).

Our understanding of annually resolved long-term European temperature variations on tree growth has consequently been restricted to a handful of TRW and MXD records from the Alps (e.g., Büntgen et al. 2005, 2006c) and Scandinavia (e.g., Briffa et al. 2001, Grudd et al. 2002, Helama et al. 2002). Because of the paucity of these reconstructions, climate conditions during the last millennium remain more uncertain and spatially less resolved than reconstructions of the past centuries. Therefore, updates of existing data and development of new data from poorly studied regions, such as the Carpathian arc, are key to understanding local- to regional-scale climatic variations, compiling larger-scale networks to assess spatial patterns of climatic change, and providing validations of climate model simulations (Esper et al. 2005b, Hegerl et al. 2006).

In this paper, we introduce a tree-ring network from the greater Tatra region within the western Carpathian arc that extends into the 21st century. We analyzed this network to evaluate tree growth responses to climate patterns, considering the influences of species (spruce, larch, fir, pine), elevation (800–1550 m a.s.l.), parameter (TRW and MXD), frequency (inter-annual and decadal scales), site ecology (luff or lee) and previous- and current-year climatic conditions (temperature and precipitation). Two multi-centennial-long temperature reconstructions based on TRW and MXD were developed for the region and compared with findings from the Alps and Central Europe. We provide details on physiologically induced response variations in the network's growth-climate relationship, and on temporal deviations between the reconstructed temperature histories.

## Data and methods

### Geographical settings

The study considers the greater Tatra region extending across

48–50° N and 19–21° E. This region includes the highest range of the western Carpathian arc and the Tatra Mountains (Figure 1). The border area between Poland and Slovakia is characterized by montane to sub-alpine forest stands with physiological and genetic differentiation between populations from higher and lower elevations (Oleksyn et al. 1998). The climate-driven treeline is situated around 1550 m a.s.l., and includes partly natural ecotones with individual conifers reaching ages of 350–450 years (Figure 2). Several mountain peaks are > 2,500 m a.s.l. Soil conditions differ among the sample sites, with a tendency for decreasing depths and increasing organic matter content with increasing altitude.

Synoptically, the North Atlantic Oscillation and Siberian High dominate during winter, whereas more localized low pressure cells occur during summer (Hurrell et al. 2003, Raible et al. 2006). Main atmospheric flows are maritime westerlies with secondary airflows from the north (Niedzwiedz 1992). The local topography results in distinct luff and lee conditions (Figure 1), with greater precipitation on the north sides of the mountain ranges (Konček et al. 1974). Mean annual temperature and precipitation over the greater Tatra region for the period 1901–2002 was 6.5 °C and 849 mm, respectively (Figure 1).

### Tree-ring data and detrending

Tree-ring data from 24 forest stands within the greater Tatra region were combined (Figure 1). These sites are distributed throughout five National Parks: *Babia Gora*, *Gorce*, *Tatra* in southern Poland and *High-* and *Low-Tatra* in Slovakia, and one National Reserve: *Pilsko*. The network comprises 1183 TRW measurement series from four conifer species, *Picea abies* (L.) Karst., *Larix decidua* Mill., *Abies alba* (L.) Karst., and *Pinus mugo* L. (herein abbreviated PCAB, LADE, ABAL and PIMU), all from elevations between 800 and 1550 m a.s.l. Datasets were developed on a site-by-site basis (Table 1), and 153 MXD series from three PCAB (7, 9 and 11) sites and one LADE (13) site were also measured. Most of the larger site collections include juvenile to mature trees (Figure 2). The mean number of rings per core sample was 128 years with a minimum of 17 years and a maximum of 442 years. The mean number of cores (each core sample represents one tree) considered per site was 48 with a minimum of 10 samples and a maximum of 128 samples. For all data, mean annual width and density were 1.37 mm year<sup>-1</sup> and 0.78 g cm<sup>-3</sup>, respectively.

For analyses and visualization, we categorized the network into high (> 1350 m), medium (> 1250 m and < 1350 m) and low (<1250 m) elevational belts. The network is characterized by 12 sites located at high elevation, from which nine are PCAB. The MXD measurement series are all derived from sites near the timberline between 1450 and 1500 m a.s.l. Six TRW sites are located at low elevation, and the remaining seven sites at medium elevation. Twenty-three sites are located in the High Tatra Mountains, two in the more southern Low Tatra Mountains and one each from the more northern Pilsko, Babia Gora and Gorce Mountains, respectively. Most of the sites in the High Tatra Mountains are located on the northern

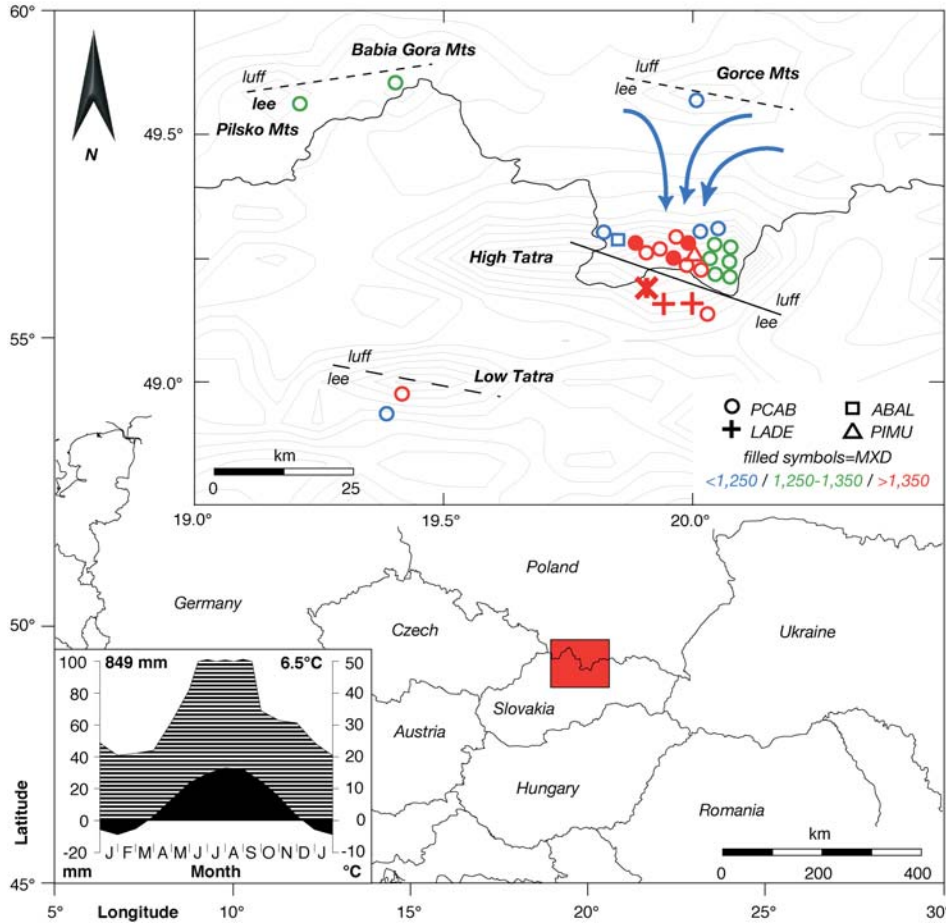


Figure 1. Location of the greater Tatra region (48–50° N and 19–21° E), with inset detailing the 24 tree-ring width (TRW) and four maximum latewood density (MXD) sampling sites, differentiated by species, parameter and elevation. The climate histogram shows the 1901–2002 monthly temperature means and precipitation sums averaged over the greater Tatra region. Arrows indicate the dominant airflow. Abbreviations: PCAB, *Picea abies*; LADE, *Larix decidua*; ABAL, *Abies alba*; and PIMU, *Pinus mugo*.

luff side, with two LADE (one containing MXD data) and one PCAB site situated on the southern lee side. The single ABAL site is located on the northwestern luff side of the High Tatra

Mountains at 1050 m a.s.l. The PIMU chronology represents uppermost treeline conditions.

To remove non-climatic biological age trends (Fritts 1976)

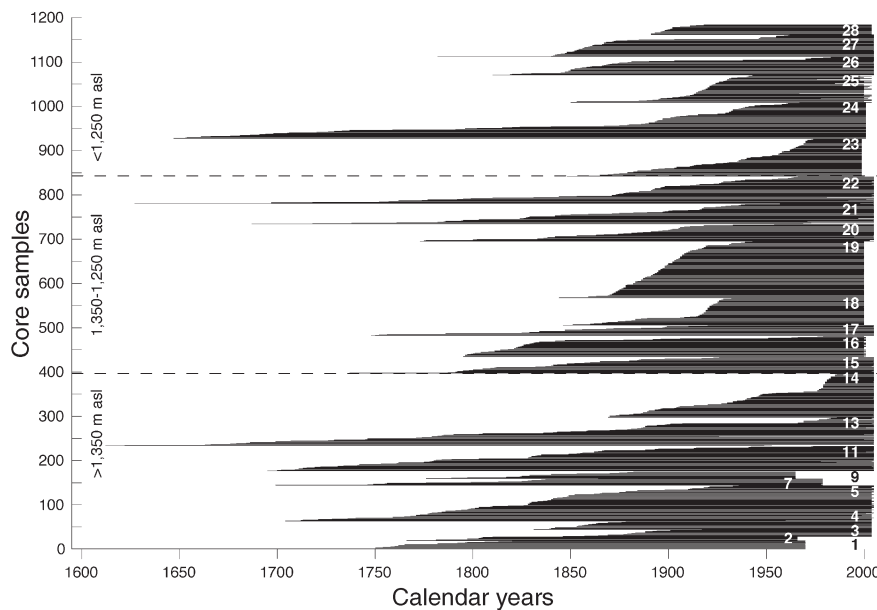


Figure 2. Sample distribution of the 24 tree-ring width (TRW) site chronologies. Additional maximum latewood density (MXD) measurements were available from four sites (7, 9, 11, 13). Each horizontal bar represents one of the 1183 core samples. The horizontal dashed lines denote site locations >1350, between 1250–1350, and <1250 m a.s.l. See Table 1 for a description of the chronologies.

Table 1. Characteristics of the 24 tree-ring width (mm) and 4 maximum latewood density ( $\text{g cm}^{-3}$ ) chronologies. Statistics refer to chronologies after power transformation, 300-year spline detrending, and truncation at  $< 5$  series. Bold lines denote MXD data. Elevation = m a.s.l., Period = full length/after truncation  $< 5$  series, MSL = mean segment length (years), MGR = mean growth rate (TRW = mm, MXD =  $\text{g cm}^{-3}$ ), and EPS (expressed population signal) = calculated over 30 years lagged by 50%, L-1 = first year autocorrelation, PC-L = PC loading, Response = highest monthly correlation with T (temperature) and P (precipitation) over the 1901–2002 or full period of overlap and Bold = MXD measurements. Identities of numbered sites: 1 = Sucha Kasprowa; 2 = Hala Gasienicowa; 3 = Nova Polianka; 4 = Nova Polianka; 5 = Zolta Turnia; 6 = Swistowko Wyznig; 7 = Swistowko Wyznig; 8 = Gasienicowy; 9 = Gasienicowy; 10 = Dolina Sucheje Wody; 11 = Dolina Sucheje Wody; 12 = Dolina Mengusowska; 13 = Dolina Mengusowska; 14 = Kosodrevina; 15 = Dolina Panszczycka; 16 = Roztoki Woloszyn; 17 = Dolina Waksmundzka; 18 = Rybiego Potoku Wlosienica; 19 = Roztoki Nowa Roztoka; 20 = Dolina Rybiego Potoku; 21 = Babia Gora; 22 = Pilsko; 23 = Roztoki Dobra Woda; 24 = Roztoki Podczub; 25 = Gorce; 26 = Dolina Chocholowska; 27 = Dolina Chocholowska; and 28 = Tale.

Site	Species	Lat/Long	Elevation	Series	Period	MSL	MGR	Rbar	EPS	L-1	PC-L	Response
1	PIMU	49°14'/20°00'	1,550	19	1742/1754–1969	195	0.28	0.38	0.9	0.71	PC1	T/Jul/.54
2	PCAB	49°15'/20°00'	1,550	10	1766/1802–1965	172	0.25	0.51	0.85	0.4	PC1	T/Jun/.36
3	PCAB	49°09'/20°10'	1,550	16	1846/1869–2003	123	1.24	0.4	0.91	0.41	PC4	T/Jun/.34
4	LADE	49°09'/20°10'	1,550	18	1831/1842–2003	149	0.89	0.63	0.97	0.42	PC3	T/May/.31
5	PCAB	49°15'/20°01'	1,500	82	1538/1721–2004	182	0.95	0.34	0.93	0.53	PC1	T/Jun/.51
6	<b>PCAB</b>	<b>49°15'/19°55'</b>	<b>1,500</b>	<b>15</b>	<b>1699/1756–1978</b>	<b>186</b>	<b>0.77</b>	<b>0.6</b>	<b>0.93</b>	<b>0.18</b>	<b>PC4</b>	<b>T/Aug/.59</b>
7	PCAB	49°15'/19°55'	1,500	15	1699/1756–1978	186	0.87	0.44	0.89	0.57	PC1	T/Jul/.43
8	<b>PCAB</b>	<b>49°14'/20°00'</b>	<b>1,500</b>	<b>16</b>	<b>1776/1824–1964</b>	<b>130</b>	<b>0.74</b>	<b>0.63</b>	<b>0.96</b>	<b>0.12</b>	<b>PC4</b>	<b>T/Aug/.58</b>
9	PCAB	49°14'/20°00'	1,500	16	1776/1824–1964	130	1.21	0.41	0.9	0.47	PC1	T/Jun/.34
10	<b>PCAB</b>	<b>49°15'/20°02'</b>	<b>1,480</b>	<b>58</b>	<b>1628/1709–2004</b>	<b>198</b>	<b>0.72</b>	<b>0.46</b>	<b>0.95</b>	<b>0.25</b>	<b>PC4</b>	<b>T/Aug/.61</b>
11	PCAB	49°15'/20°02'	1,480	58	1628/1709–2004	198	0.78	0.36	0.93	0.59	PC1	T/Jun/.53
12	<b>LADE</b>	<b>49°09'/20°04'</b>	<b>1,450</b>	<b>64</b>	<b>1612/1676–2004</b>	<b>166</b>	<b>0.89</b>	<b>0.46</b>	<b>0.95</b>	<b>0.23</b>	<b>PC3</b>	<b>T/Jul/.47</b>
13	LADE	49°09'/20°04'	1,450	64	1612/1676–2004	166	0.97	0.58	0.97	0.38	PC3	T/May/.30
14	PCAB	48°56'/19°36'	1,450	100	1869/1873–2004	63	2.03	0.35	0.96	0.63	PC5	T/Jul/.33
15	PCAB	49°15'/20°02'	1,420	36	1737/1792–2004	165	1.1	0.32	0.92	0.63	PC1	T/Jun/.43
16	PCAB	49°14'/20°04'	1,370	47	1795/1796–2000	161	1.16	0.32	0.94	0.54	PC1	T/Jun/.39
17	PCAB	49°15'/20°04'	1,350	24	1748/1777–2004	169	1.08	0.27	0.82	0.58	PC1	T/Jul/.41
18	PCAB	49°13'/20°05'	1,330	62	1846/1862–1999	93	1.43	0.31	0.93	0.72	PC3	T/Jul/.28
19	PCAB	49°14'/20°05'	1,310	128	1844/1863–1999	105	1.28	0.35	0.98	0.59	PC4	P/Mar/.21
20	PCAB	49°14'/20°05'	1,300	39	1773/1802–2004	132	1.53	0.24	0.82	0.67	PC4	T/Jun/.31
21	PCAB	49°35'/19°30'	1,300	46	1687/1782–2004	143	1.67	0.39	0.93	0.69	PC1	T/Jul/.43
22	PCAB	49°31'/19°20'	1,300	61	1627/1752–2004	133	1.74	0.33	0.92	0.62	PC4	T/Jul/.40
23	PCAB	49°14'/20°05'	1,230	86	1848/1865–1998	65	1.8	0.27	0.92	0.66	PC4	P/Dec/.29
24	PCAB	49°14'/20°05'	1,210	81	1647/1661–2000	150	0.72	0.38	0.93	0.71	PC1	T/Jun/.28
25	PCAB	49°33'/20°08'	1,100	62	1850/1885–2003	84	2.57	0.39	0.96	0.83	PC1	T/Jul/.42
26	ABAL	49°17'/19°50'	1,050	42	1810/1830–2004	126	1.16	0.34	0.93	0.84	PC5	P/Jul/.26
27	PCAB	49°17'/19°50'	1,000	50	1782/1842–2004	129	1.53	0.37	0.96	0.86	PC5	T/Mar/.30
28	PCAB	48°52'/19°36'	800	22	1891/1894–2003	103	2.03	0.38	0.91	0.81	PC4	P/Jun/.32

from the TRW and MXD measurement series (Figure 3), an adaptive power transformation was first applied to reduce the heteroscedastic behavior of the TRW measurement series (Cook and Peters 1997). Indices of both the TRW and MXD series were then taken as residuals from cubic smoothing splines with the 50% frequency-response cutoff at 300 years (Cook and Peters 1981). This approach emphasized inter-annual to multi-decadal scale variations. Longer-term growth trends, however, were removed (Cook et al. 1995). Measurement series were averaged to form chronologies on a site-by-site basis based on a bi-weight robust mean. Chronologies had their variance stabilized for changes in sample size by methods introduced by Osborn et al. (1997), and then truncated at a minimum sample size of  $< 5$  series. The common period for all 28 chronologies is 1894–1964 after truncation (Table 1, Figure 2). With 14 chronologies originating before 1800, and 19 chronologies extending into the 21st century, this current network represents a significant update of the six pio-

neering western Carpathian chronologies developed in the 1960s and 1970s (see Bednarz 1984 for details). After aligning the chronologies' raw measurement series by their cambial age (Esper et al. 2003), the resulting Regional Curves (RCs) describe mean growth trends for the given site and species within the network (Figure 3). These age trends were predominantly related to elevation, because lower-elevation sites generally show wide juvenile rings, whereas juvenile growth at higher elevations is typically more depressed.

Signal strength of the site chronologies was assessed by the inter-series correlation (Rbar), and the Expressed Population Signal (EPS) statistics computed in moving windows (Wigley et al. 1984). Relevant chronology characteristics and statistics are listed in Table 1. The Rbar and EPS statistics of the site chronologies signal strength ranged from 0.24 to 0.63 and from 0.82 to 0.98, respectively (Table 1). Except for two PCAB chronologies (17 and 20), EPS values were above the frequently applied threshold of 0.85 indicating robust mean-

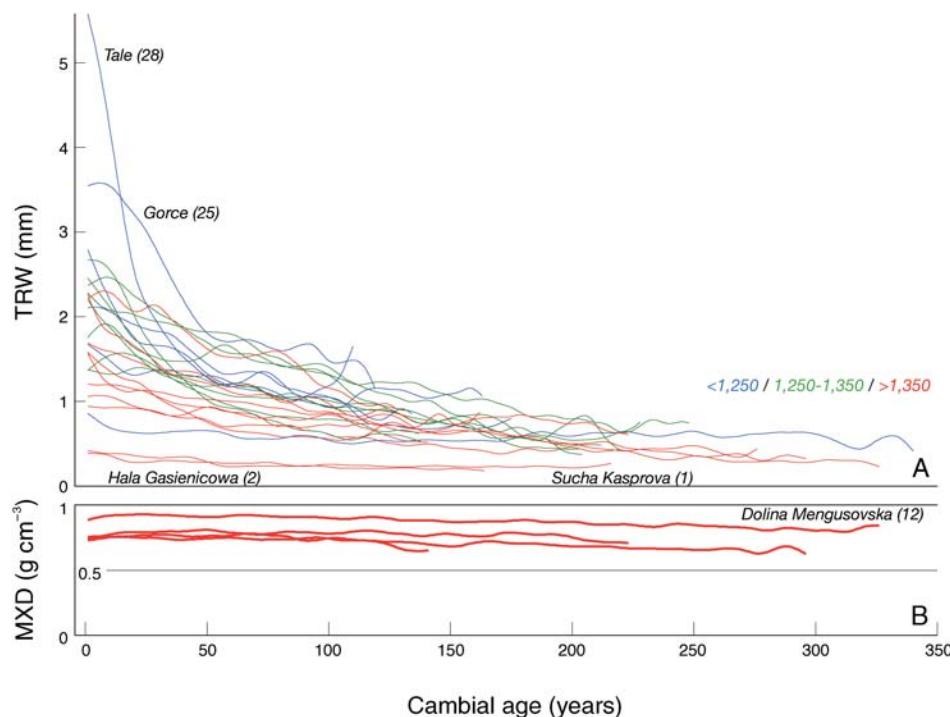


Figure 3. Mean growth trends of (A) the 24 tree-ring width (TRW) and (B) the four maximum latewood density (MXD) chronologies after aligning all measurement series by cambial age. Average series (Regional Curves, RCs) are 20-year low-pass filtered and truncated at < 5 series. Names and numbers refer to the site chronologies as listed in Table 1.

value functions (Wigley et al. 1984). Lag-1 autocorrelations of the 24 TRW and four MXD chronologies ranged from 0.40 to 0.86 and from 0.12 to 0.25, respectively. This lower persistence of previous-year growth conditions in the MXD data reflects the reduced biological memory of this parameter (e.g., Frank and Esper 2005a). The lag-1 autocorrelations of the “target” monthly temperature means and precipitation sums ranged from -0.02 to 0.26 and from -0.19 to 0.13, respectively.

Correlations between the four TRW and MXD chronology pairs from the same sites were lower for the three PCAB pairs and higher for the LADE pair (Table 2). We assume this is related to a higher sensitivity of radial growth and lower biological memory of LADE (see Table 1). The periodic occurrence of annual growth depressions caused by larch budmoth (*Zeiraphera diniana* Gn.) population outbreaks, commonly reported for the European Alps (Baltensweiler and Rubli 1999), however, can be excluded for the Tatra Mountains LADE trees. The relatively low within-site correlations of PCAB suggest that TRW and MXD contain different environmental or

climatic signals, or both (see below PC loadings of the individual chronologies).

*Meteorological data*

For growth response and calibration analyses, a dataset of gridded (0.5° × 0.5°) monthly temperature and precipitation series was used (CRU TS 2.1, Mitchell and Jones 2005). Temperature data from 16 grid-boxes that cover the 48–50° N and 19–21° E region and 1901–2002 period were expressed as anomalies with respect to the 1961–1990 mean. Correlation analysis between the 28 tree-ring chronologies and climate data was undertaken over the 1901–2002 period, or for the individual maximum period of overlap for chronologies that end before 2002, using an 18-month window from May of the year prior to tree growth until the current-year October. Temperature means and precipitation sums are for the periods February–April, April–September, March–September, June–September, April–August, March–August, June–August and June–July. Time periods of < 10 and > 10 years are denoted as high and low frequency, respectively, and significance levels

Table 2. Correlations between the four tree-ring width and maximum latewood density chronology pairs, using their original, 10-year high-, and low-passed components over the individual periods of overlap. Parenthesis denote correlations computed over the 1824–1964 common period. Abbreviations: PCAB, *Picea abies*; and LADE, *Larix decidua*.

Chronology	PCAB			LADE
	6/7 Swistowko Wyznig	8/9 Gasienicowy	10/11 Dolina Suchej Wody	12/13 Dolina Mengusovska
Original	0.37 (0.28)	0.17 (0.17)	0.31 (0.20)	0.63 (0.72)
High-passed	0.21 (0.16)	0.18 (0.18)	0.17 (0.11)	0.65 (0.67)
Low-passed	0.54 (0.46)	0.18 (0.18)	0.51 (0.38)	0.65 (0.83)

conservatively corrected for lag-1 autocorrelation (Trenberth 1984) using the monthly values with highest autocorrelations for the confidence adjustment of all correlations.

## Results

### Growth response to climate

Correlation analysis of the TRW site chronologies to temperature revealed a rather consistent response to current-year June and July temperatures (Figures 4A and 4B), with the exception

that the lowest elevation sites deviated from this pattern and showed an inverse behavior. The TRW correlations with August temperatures were not significant ( $P > 0.05$ ), whereas the TRW correlations with current-year late winter–early spring temperatures were generally positive for lower elevation sites, including some significant ( $P < 0.05$ ) responses to February, March and April temperatures. Chronologies from higher elevations generally showed a negative response to March and April temperatures. Several chronologies from higher elevations also had positive correlations ( $P < 0.05$ ) with previous-year October and November temperatures, a feature com-

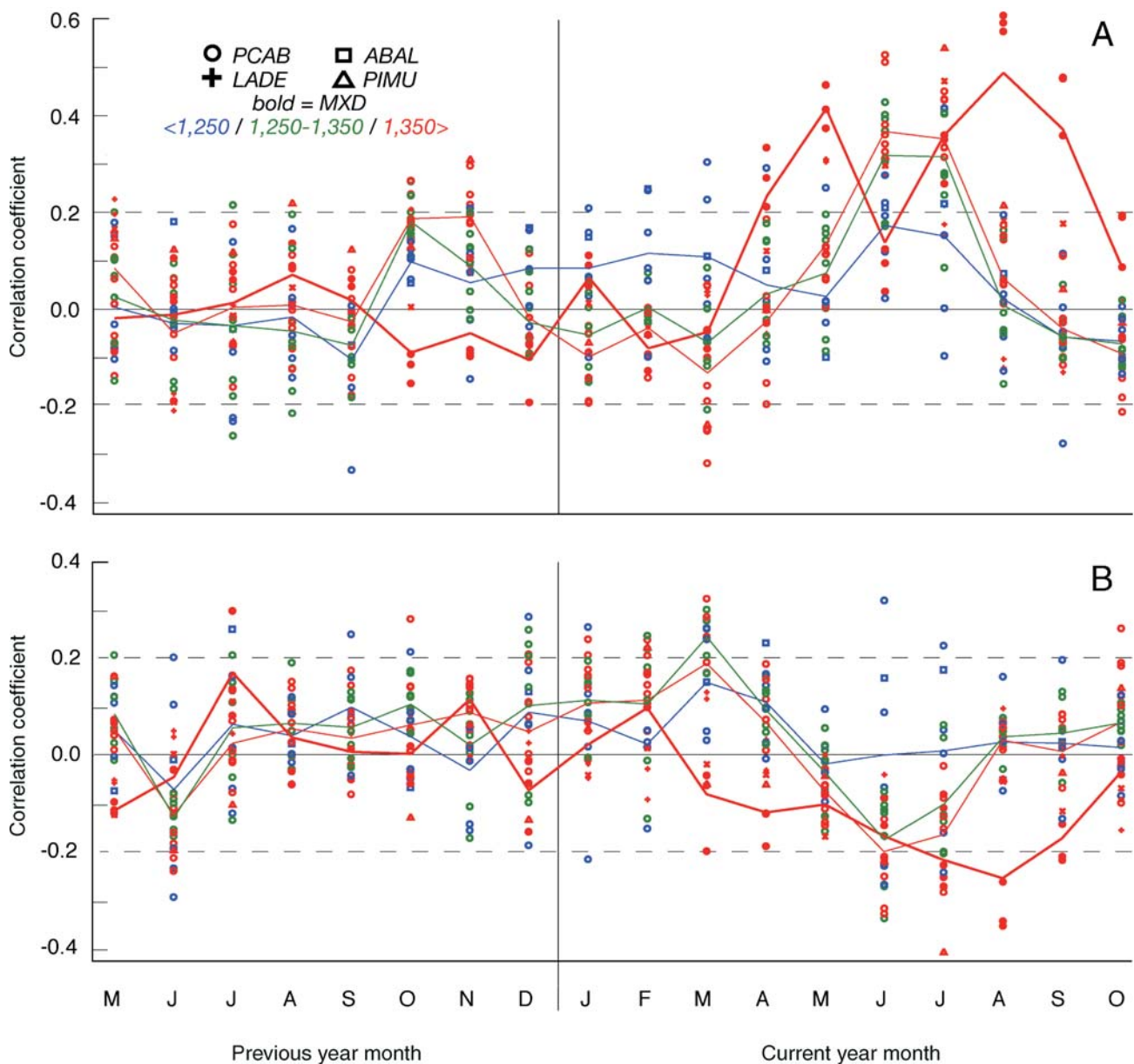


Figure 4. Monthly growth response of the 28 chronologies to (A) temperature means and (B) precipitation sums over the 1901–2002 period. Thin lines indicate mean elevations and the bold lines indicate maximum latewood density (MXD) means. Correlations were computed from previous-year May to current-year October. Horizontal dashed lines denote 95% significance, corrected for lag-1 autocorrelation (Trenberth 1984), using the monthly mean autocorrelation. The vertical line indicates the beginning of the current growth year. Blue, green and red colors refer to elevations < 1250, 1250–1350 and > 1350 m a.s.l., respectively.

monly reported from the European Alps (Oberhuber 2004, Frank and Esper 2005a). Although almost all TRW records showed no significant correlations with previous-year summer temperatures, TRW at some lower elevation sites correlated negatively ( $P < 0.05$ ) with July, August and September temperatures of the year before ring formation.

The four MXD sites were dominated by positive correlations ( $P < 0.05$ ) with March, April, July, August and September temperatures, but there were no significant correlations with previous-year May to current-year March temperatures. The MXD correlations with June temperatures of the growth year were low. A similar monthly optimum of MXD formation is reported from a LADE MXD network from nearby timberline sites in the central Swiss Alps (Büntgen et al. 2006c), and from a multi-species analysis of high-elevation sites across the Alpine arc (Frank and Esper 2005a).

The TRW response pattern to precipitation was generally opposite to the correlations with temperature (Figure 4B). Although TRW commonly correlated positively with spring precipitation (particularly March), MXD showed a negative response to spring precipitation. The correlations for TRW and summer precipitation were generally negative, with some significant negative correlations ( $P < 0.05$ ) for June and July. Negative correlations ( $P < 0.05$ ) with summer precipitation (June, July, August and partly September) were also pronounced for the MXD chronologies. Some positive correlations ( $P < 0.05$ ) were obtained between June and July precipitation sums and the TRW of the network's lowest site chronology (28), at about 800 m a.s.l. south of the Low Tatra Mountains.

Based on these monthly correlation results, we calculated seven seasonal temperature means for the period from April to September for comparison with the 28 site chronologies. Accordingly, 20 TRW chronologies correlated significantly with June–July temperatures, whereas the MXD chronologies had the strongest response to the longer April–September season (Figure 5). These results demonstrate the more integrative nature and slightly higher climate sensitivity of the MXD data compared with the TRW data. The decreasing growth response to summer season temperatures with decreasing elevation is indicated by the two lower elevation TRW chronologies that did not correlate significantly with any seasonal mean, and the lowest site chronology (28) that showed negative correlations.

For a better understanding of these relationships, the tree-ring and meteorological data were decomposed into high- and low-pass components. Probability distribution functions of these data showed greater coherency in the higher frequency domain (Figure 6A). Analysis of these frequency-dependent correlations as a function of elevation revealed significant ( $P < 0.01$ ) dependency for the original and high-pass chronologies and nonsignificant results for the low-pass component (Figure 6B). Although the network's elevational gradient is only 750 m (800–1550 m a.s.l.), these frequency-specific vertical correlation patterns indicate that a stronger temperature signal is preserved toward the upper growth limit, particularly for the inter-annual domain.

*Principal component analysis*

Principal component analysis (PCA) was performed to seek

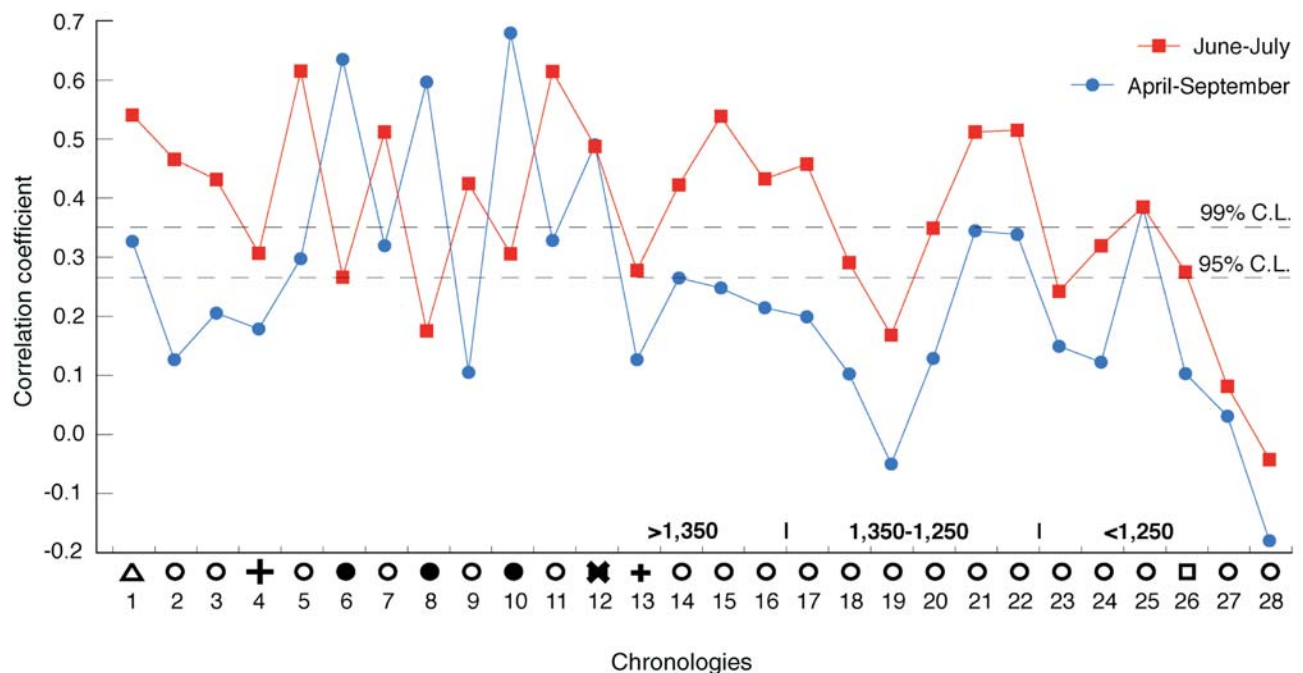


Figure 5. Growth responses to temperature variation of the 28 chronologies computed against the seasonal temperature means of June–July (red) and April–September (blue) over the 1901–2002 period.

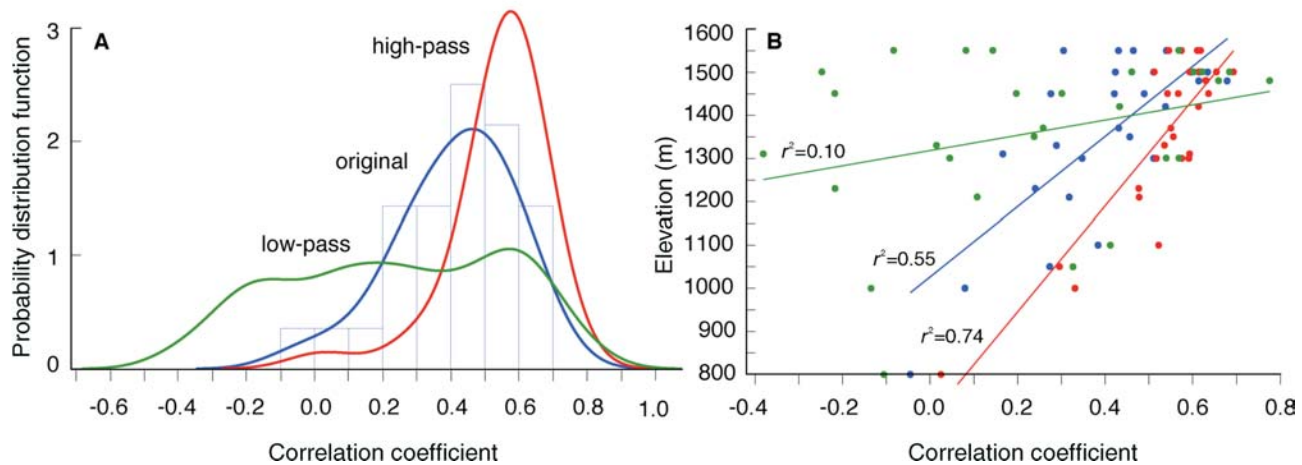


Figure 6. (A) Frequency-dependent growth responses to temperature variation of the 28 chronologies computed over the 1901–2002, or individual maximum period of overlap, using the original (blue), high-pass (red), and low-pass (green) chronologies. The light blue histogram shows the distribution of the original data and is plotted along with estimates of the probability distribution function for the original, high- and low-pass data derived using a Kernel filter. The 24 tree-ring width site chronologies are correlated against June–July temperature means, whereas the four maximum latewood density chronologies are correlated against April–September means. (B) Comparison of the frequency dependent seasonal correlations as a function of elevation.

homogeneity within heterogeneity, as data subsets with optimized signal coherency are created and patterns inherent in the network detected (Peters et al. 1981). Based on the 1894–1964 period shared by all 28 chronologies, the first principal component (PC) explained 42% and the first seven PCs explained 84% of the network's variance. The first seven PCs with eigenvalues greater than unity were retained for varimax rotation (Richman 1986). Resulting clusters became even more apparent after using the first five PCs (eigenvalues > 1.5) containing 76% of the variance (Figures 7A and 7B). Chronology grouping depended on a combination of species, parameter and elevation, but was slightly diminished by ecological site condition (Table 1).

To differentiate the climatic signal preserved by the five rotated PCs, analyses were repeated over the 1901–1978 period and correlated against monthly and seasonal temperature means and precipitation sums (Figure 8). This analysis period is a compromise between the number of site chronologies entering the PCA (24 chronologies) and the operational window length (78 years). Principal component 1, mainly integrating high-elevation PCAB TRW data, correlated positively ( $P < 0.05$ ) with June–July temperatures. Principle component 4, mainly integrating high-elevation MXD data, showed the overall highest correlations ( $P < 0.05$ ) with monthly August and seasonal April–September temperatures. Principal component 2 correlated negatively ( $P < 0.05$ ) with previous-year

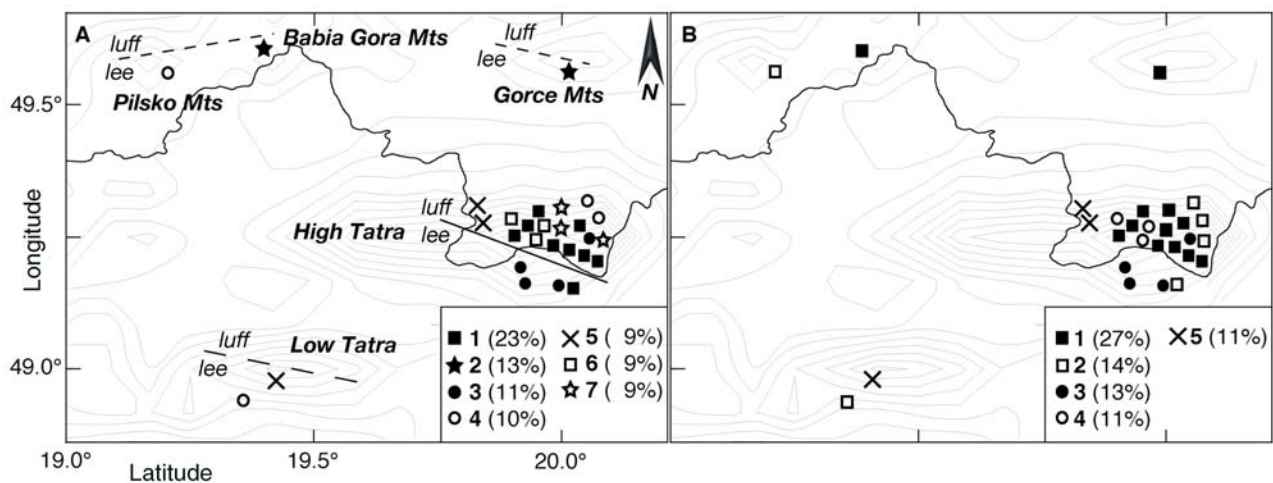


Figure 7. Loadings of the 28 chronologies on the (A) first seven and (B) first five varimax-rotated principal components (PC), based on the 1894–1964 common period. Parentheses indicate the explained amount of variance of each PC eigenvector. Varimax loadings of each chronology on the eigenvector on which it most strongly weights ranged from 0.42–0.97 (0.52–0.97), with a mean of 0.76 (0.75) when using the first seven (five).

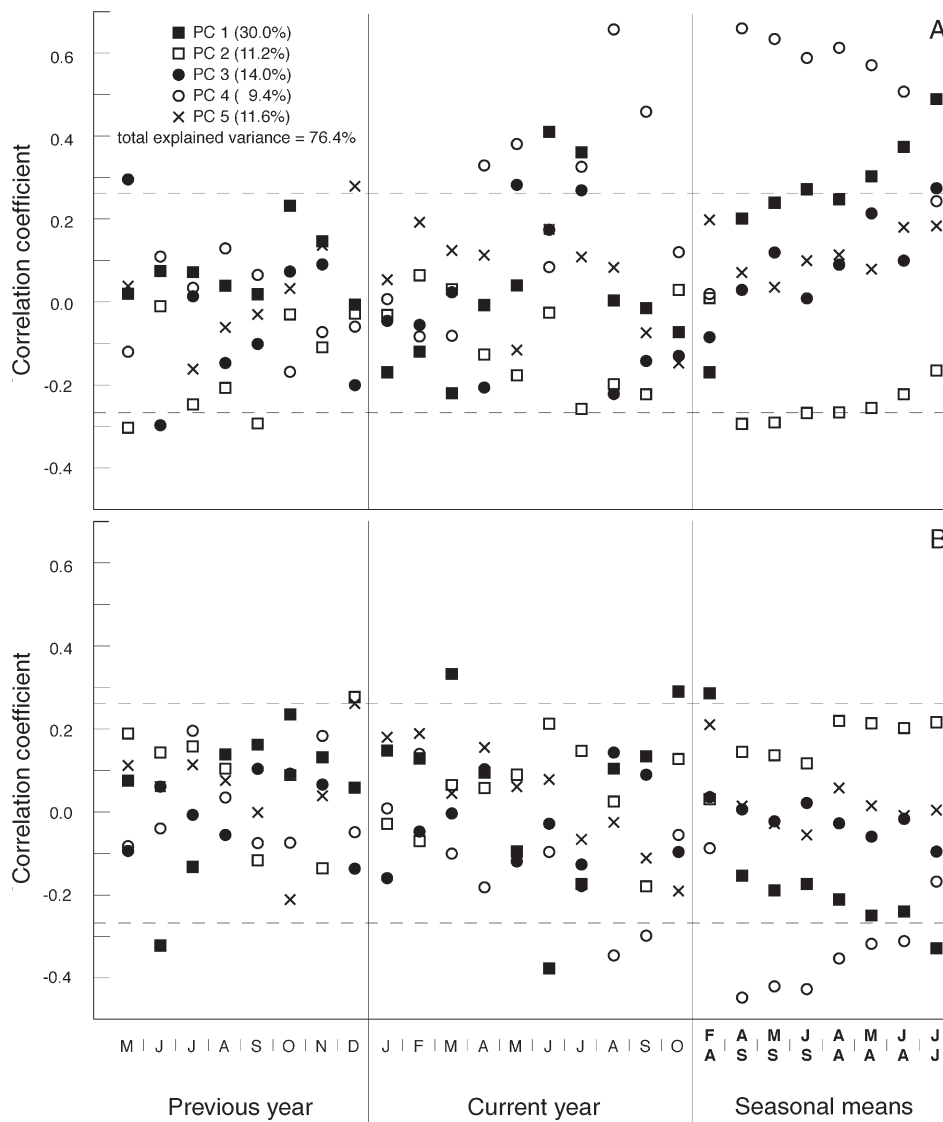


Figure 8. Monthly and seasonal correlations between the five rotated PCs and (A) temperature means and (B) precipitation sums computed over the 1901–1978 period. Horizontal dashed lines denote 95% significance. Monthly abbreviations refer to the 18-month window from previous-year May to October of the growth year, and the seasonal means: February–April, April–September, May–September, June–September, April–August, May–August, June–August and June–July.

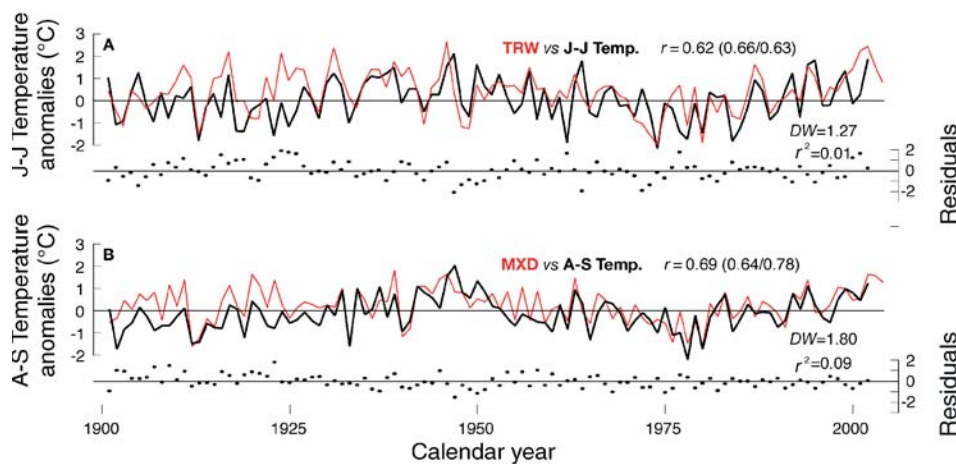


Figure 9. Comparison of the actual (black) and predicted (red) temperatures, after scaling (A) the tree-ring width (TRW)-based mean chronology against June–July temperatures, and (B) the maximum latewood density (MXD)-based mean chronology against April–September temperatures (1901–2002). Temperatures are expressed as anomalies from the 1961–1990 mean. Correlations were significant at the 99.9% confidence level, and scatter plots indicate the model residuals, with the Durbin–Watson (DW) statistic and the linear trend of the residuals shown.

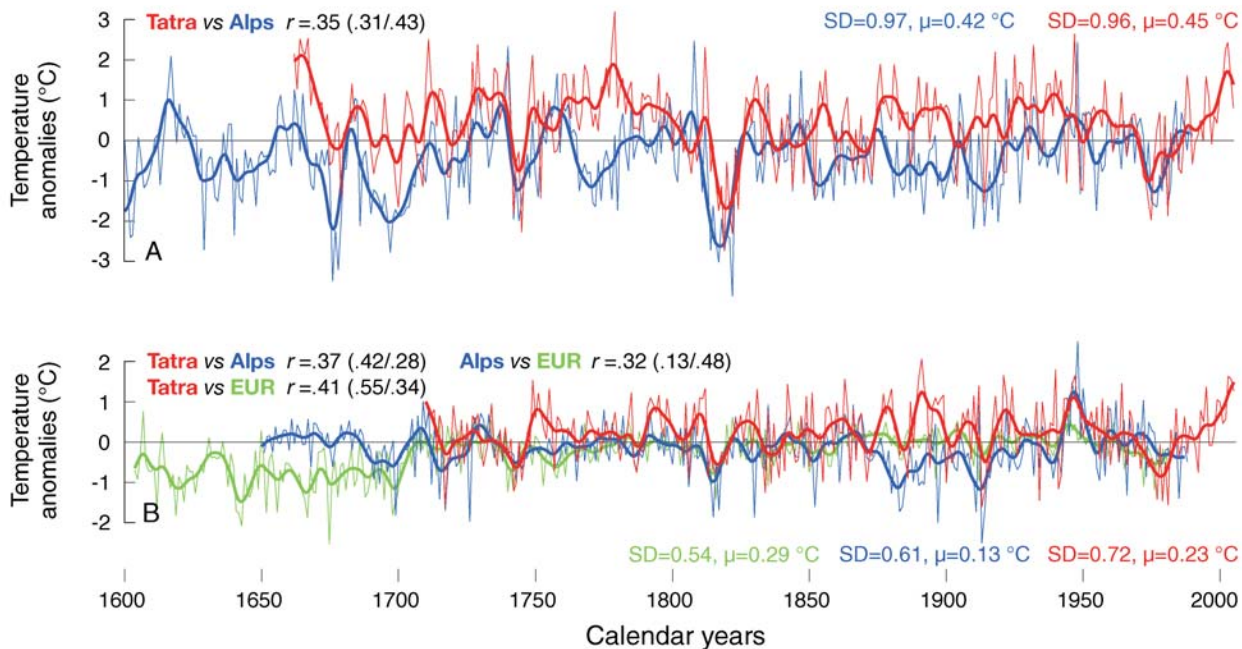


Figure 10. Comparison of (A) the tree-ring width- and (B) the maximum latewood density-based Tatra June–July and April–September temperature reconstructions (red) with the June–August and April–September Alpine temperature reconstructions by Frank and Esper (2005) (blue), and the April–September Central European temperature reconstruction by Briffa et al. (2001) (green). Smoothed lines are 10-year low-pass filters. Standard deviation (SD) and mean ( $\mu$ ) of the original reconstructions are shown. The Tatra and Central European reconstructions are expressed as anomalies from the 1961–90 mean, whereas the Alpine reconstructions are expressed as anomalies from the 1901–1998 mean. Parentheses denote correlations derived from the 10-year high- and low-pass chronologies, respectively.

March and September temperatures and current-year April–September and March–September temperatures. Correlations for PC3 and PC5 were all nonsignificant.

#### Temperature reconstructions

For temperature reconstruction, we considered the arithmetic means of the chronologies that loaded most strongly on either PC1 or PC4 (Figure 9). Accordingly, the mean of the 11 PCAB and one PIMU TRW chronologies ( $\sim$ PC1) showed the strongest response to peak summer June–July temperatures ( $r = 0.62$ ;  $P < 0.001$ ), and the mean of the three PCAB MXD chronologies ( $\sim$ PC4) showed the strongest response to the wider April–September season ( $r = 0.69$ ;  $P < 0.001$ ). No correlations with the previous-year climate and the current-year precipitation measurements were significant ( $P > 0.05$ ).

To avoid loss of amplitude as a result of regression error (Esper et al. 2005a), a simple scaling of the mean chronologies to the meteorological target data was applied, i.e., the variance and mean of the chronologies were set equal to those of the instrumental “target” data over the 1901–2002 period (Figure 9).

The TRW-based June–July and MXD-based April–September reconstructions explained 39 and 48% of the regional temperature variability, respectively. Actual and predicted records indicated a linear relationship, with both reconstructions modeling high- and low-frequency variations reasonably well (Figure 9). Durbin–Watson values (DW, Durbin and Watson 1951) of 1.27 and 1.80 computed over the 1901–2002 period

of overlap assessed the reconstructive accuracy of the TRW- and MXD-based reconstructions, respectively. Split period calibration and verification tests were performed over the 1901–1951 and 1952–2002 windows to prove the model’s temporal stability. Reduction of error (RE) values were 0.11 and 0.38 for the 1901–1951 and 1952–2002 periods, and the corresponding coefficient of efficiency (CE) values were 0.10 and 0.37, respectively. These statistics demonstrate that useful temperature information is preserved in the models (Cook et al. 1994). The June–July and April–September Tatra temperature reconstructions cover the periods 1661–2004 and 1709–2004, respectively. They correlate at 0.33, 0.46 and 0.24 based on their original, high- and low-pass components, respectively, over the 1709–2004 period of overlap. Common features include temperature increases from  $\sim$ 1900 to 1950, decreases from  $\sim$ 1950 to 1980, and recent increases from  $\sim$ 1980 to the present. The April–September reconstruction showed less amplitude than the June–July reconstruction, as indicated by the standard deviations (Figure 10). Similarly, standard deviations of the instrumental data, calculated over the 1901–2002 period, were higher for June–July (0.95) than for April–September (0.77).

#### Discussion and conclusions

##### Growth responses to climate variations

Although the growth responses to climate revealed by the 28 chronologies support common knowledge, such as temper-

ature sensitivity toward higher elevations and drought-stress toward lower elevations, and within species coherency (e.g., Tranquillini 1964, Fritts 1976, Körner 1998), some features were discerned.

(1) Positive correlations between TRW and previous-year autumn temperatures suggest that warm October and November conditions likely support carbon storage, promote mycorrhizal root growth by maintaining soils above freezing, and favor maturation of needles, shoots and buds against early winter stress (Oberhuber 2004). These factors, in combination with sufficient water supply promote early wood cell formation during spring. This physiological requirement seems to be important for TRW formation, because significant correlations with previous-year climate are also reported from numerous TRW chronologies across the European Alps and northern latitudes (see studies cited in the Introduction). In contrast, previous-year effects tended to be minimal for the formation of MXD (Briffa et al. 2002, Büntgen et al. 2005, Frank and Esper 2005a).

(2) Negative correlations between TRW and MXD and early spring (February–March) temperatures likely reflect the protective character of winter snow cover at high elevations (Vaganov et al. 1999). Oberhuber (2004) described the tendency of trees at the alpine timberline to suffer from enhanced desiccation as a result of increased transpiration rates of needles and shoots, photoinhibitory stress and short-term fluctuations in shoot temperatures, during winter–early spring periods with insufficient snow depth.

(3) A lower correlation between MXD and June temperatures compared with the surrounding months, which is also reported from some MXD chronologies across the European Alps and northern latitudes (Briffa et al. 2002, Frank and Esper 2005a), may be associated with the production of cones or pollen, or both, instead of cell wall growth (Eis et al. 1965), and additional cellular division dominating metabolic activity. The formation of TRW, however, was positively affected by June temperatures and correlations between growth increment and June–July temperatures were highest. We assume that early wood cell production starts in April and May, followed by maximum cell production in June–July. High-resolution dendrometer point measurements showed that the stem radius increase in PCAB in Scandinavia and northeastern France starts in April and May, with the greatest daily increments being recorded in July. The production of late wood cells most likely occurs in July and August, but can extend into September (Schweingruber 1996, Mäkinen et al. 2003, Bouriaud et al. 2005). Intra-annual variations in wood density, particularly during the second half of the growing season, likely reflect changes in the accessibility of soil water caused by severe late summer drought stress (Bouriaud et al. 2005, Kahle 2006).

(4) Positive correlations and a maximum TRW response to June–August temperatures have been found in numerous high-elevation sites across the Alpine arc (Büntgen et al. 2005, Frank and Esper 2005a). In contrast, correlations between TRW and August temperatures were not significant in the Tatra Mountains, likely resulting from the prevailing colder or drier climatic conditions, or both, during the late summer–au-

turn transition. This regional finding is supported by numerous TRW site chronologies across the Eurasian high northern latitudes that do not significantly correlate with August temperatures (Briffa et al. 2002).

(5) Generally negative correlations with previous-year June precipitation were obtained for TRW and MXD, likely reflecting a carry-over effect (Fritts 1976). Growth variations result from the persistence of various effects into subsequent years through changes in nutrients and biological preconditioning of growth. For most conifers, the carry-over effect, such as photosynthetic gain, and storage of assimilates and water from the previous growing season, impacts current-year radial growth (Kozłowski and Pallardy 1997).

(6) Positive correlations between TRW and March precipitation indicated the importance of water supply during the first part of the growing season. A combination of precipitation, temperature and the timing of snow melt is likely responsible for this key period of early wood production (Vaganov et al. 1999), which then dominates total annual ring diameter.

(7) Highest positive correlations were found between April–September temperatures and MXD, and between June–July temperatures and TRW, so the reverse response to precipitation indicated a negative correlation between temperature and precipitation during the summer months. The general climatic response of the TRW chronologies compared with their MXD counterparts might be influenced by the tendency for greater sensitivity of current-year ring formation to biological and environmental conditions of the previous year. Severe autumn conditions in the year before ring formation caused a reduction in latewood cell wall thickness, nutrition reserve and bud production (Rolland 1993, Oberhuber 2004), resulting in diminished early wood cell formation, leaf area investment and photosynthetic capacity, and causing an overall decrease in radial growth (Schweingruber 1996). Enhanced high-frequency interannual variation in growth responses to climate variation is found in both TRW and MXD from higher elevations, with signal coherency diminishing toward lower elevations and lower frequencies.

Besides these parameter-induced features, the study revealed differentiation of the network's growth response to climate as a function of: (1) elevation; (2) species; and (3) more general ecophysiological variables.

(1) Increasing precipitation signals toward lower elevations including growth depressions as a result of drought stress were characteristic of the few sites situated ~1,000 m a.s.l. Based on the assumption that increasing temperatures lengthen the growing season by advancing snow melt (Vaganov et al. 1999), and tend to enhance photosynthesis in trees through a positively correlated increase in solar irradiance and summer temperatures, a moderate warming is likely to be beneficial at the upper timberline. Trees from lower elevations, however, are expected to respond differently, because associated secondary effects of enhanced warming, such as increased evapotranspiration and lower late summer soil water content may have more influence than temperatures alone, and will likely result in drought-stress (Leuzinger et al. 2005, Kahle 2006). Moreover, increasing photosynthesis does not translate di-

rectly into increasing growth (Chapin and Shaver 1996), and the idealized linear temperature response of high-elevation trees will collapse above some threshold.

(2) Differences in the geographical distribution of PCAB and LADE were evident. Compared with PCAB, LADE was better able to cope with drought, and therefore is restricted to the southern lee slopes of the High Tatra Mountains. PCAB, however, is found throughout the network. At around 13 °C, subalpine PCAB seems unable to take full advantage of warm sunny days (Carrer et al. 1998), perhaps because it tends to favor water storage over water uptake. At an equivalent threshold of ~16 °C, LADE, commonly situated at dryer sites, is less affected, because it develops a deep root system that provides access to the deepest and wettest soil layers (Tranquillini 1964). (Thresholds are not constant among differing site ecologies (Marco Carrer, personal communication)). Thus, a combination of higher temperatures and adequate water availability only stimulates positive radial growth below a critical threshold (D'Arrigo et al. 2004), because drought-induced disruptions in the assimilation processes likely inhibit radial growth (Anfodillo et al. 1998).

(3) General uncertainty about the observed relationships could be associated with nonlinearity in the physiological responses of trees to climate (Tranquillini 1964, Fritts 1976, Kozłowski and Pallardy 1997), growth response to maximum rather than mean temperatures (Wilson and Luckman 2003), changes in the growing season length including slow ecological shifts (Vaganov et al. 1999, Frank and Esper 2005b), and changes in the annual meteorological cycle (Jones et al. 2003). We did not observe temporal instability in the 20th century growth responses to climate (e.g., Briffa et al. 1998, Büntgen et al. 2006a), particularly at the higher elevation sites.

#### *Temperature history*

Temperature reconstructions of the greater Tatra region were compared with those obtained for the Alpine arc (Frank and Esper 2005b), and Central Europe (Briffa et al. 2001) (Figure 10). Common features included cold periods ~1650–1700 and 1810–20, associated with the Dalton and Late Maunder solar minima (Eddy 1976), and following sequences of major volcanic eruptions (Simkin and Siebert 1994). Early warm periods are commonly reconstructed ~1730 and ~1800. Temperature variations during the 20th century synchronously describe warming from around the 1910s to the 1940s, cooling in the 1970–80s, and increasing temperatures again thereafter.

Because of the inclusion of new samples in the Tatra network, the temperature reconstructions capture the last two decades of prevailing warming without instrumental splicing of the proxy into the 21st century. Lag-1 autocorrelation was 0.43 and 0.39 for the Tatra and Alpine TRW-based reconstructions, respectively, but significantly lower (0.14) for both MXD-based reconstructions, most likely because of the lower biological memory of MXD compared with TRW. Correlations between the Tatra and Alpine TRW and MXD reconstructions were 0.35 and 0.37, respectively. The high- and low-pass components indicated stronger low frequency agreement for the TRW chronology, but enhanced high frequency agreement for

the MXD chronology. In comparison, correlations between the meteorological June–July versus June–August and April–September versus April–September “target” data from the Tatra and Alps were 0.44 and 0.70, respectively. The Central European April–September reconstruction has a lower standard deviation than the corresponding MXD-based Tatra and Alpine reconstructions, likely related to the instrumental “target” used, the larger region and number of sites averaged, and the calibration model, such as regression instead of scaling, applied (Esper et al. 2005a, 2005b, Büntgen et al. 2006b). The lag-1 autocorrelation of 0.46 is clearly higher than the 0.14 obtained for the two regional MXD reconstructions. The correlation between the Tatra and Central European MXD reconstructions is 0.41. After high- and low-pass filtering, correlations increased to 0.55 and decreased to 0.34, respectively (common period). Similarly, correlations between the Alpine and Central European MXD reconstructions were 0.32, 0.13, and 0.48 for the unfiltered, high-pass, and low-pass data, respectively (common period).

Offset in the estimated long-term trends, i.e., lower in the Tatra and Alpine records and greater in the Central European record, likely results from the detrending techniques applied (Briffa et al. 2001, Frank and Esper 2005b). The Central European reconstruction is optimized for the preservation of lower frequency information, whereas the Tatra and Alpine records are limited in this respect. Temporal offset between the individual reconstructions may derive from the maritime-continental gradient between the Alps and Tatra Mountains. Longer-term changes in European atmospheric flow-regimes (Raible et al. 2006), and in the European and North Atlantic climate system are reported for past centuries (Luterbacher et al. 2004, Casty et al. 2005). Summer synoptic heterogeneity causes distinct local regimes (Hurrell et al. 2003). For example, the Central European heat wave in 2003 (Luterbacher et al. 2004, Schär et al. 2004), was less extreme in the greater Tatra region, as indicated by both meteorological measurements and tree growth.

Although regional- to continental-scale network analyses from the Alps and Central Europe support the dominant role of rather homogeneous summer season temperatures on high-elevation tree-growth, we advocate the importance of carefully selected tree-ring data and detrending methods, sufficiently large samples, and detailed growth and climate analyses before drawing climatic interpretations from the chronologies created. The network we studied could be optimized toward a more uniform distribution of species (more LADE, PIMU and ABAL sites), parameter (more MXD site chronologies) and ecology (more lower elevation sites). The reduction in sample size back in time and limited preservation of low-frequency information could be compensated by the inclusion of carefully selected historical timber samples. Enhanced understanding of the network's growth response characteristics under changing site and climate conditions could be provided by a south extension along the Carpathian arc.

#### **Acknowledgments**

We thank Z. Bednarczyk for field assistance, logistics, organization and

discussion during the project's earlier stage, T. Mitchell for providing meteorological data, and K. Briffa for making temperature reconstructions available. K. Treydte, F.H. Schweingruber and R.J.S. Wilson are thanked for comments and discussion. Supported by the SNF project Euro-Trans (No. 200021-105663), NCCR-Climatic (Extract) and the EU project Alp-Imp (No. 01.0498-1).

## References

- Anfodillo, T., S. Rento, V. Carraro, L. Furlanetto, C. Urbinati and M. Carrer. 1998. Tree water relations and climate variations at the alpine timberline: seasonal changes of sap flux and xylem water potential in *Larix decidua* Miller, *Picea abies* (L.) Karst. and *Pinus cembra* L. *Ann. Sci. For.* 55:159-172.
- Baltensweiler, W. and D. Rubli. 1999. Dispersal: an important driving force of the cyclic population dynamics of the larch bud moth. *For. Snow Landsc. Res.* 74:3-153.
- Bednarz, Z. 1984. The comparison of dendroclimatological reconstructions of summer temperatures from the Alps and Tatra Mountains from 1741-1965. *Dendrochronologia* 2:63-72.
- Bednarz, Z., B. Jaroszewicz, J. Ptak and J. Szwagrzyk. 1999. Dendrochronology of Norway spruce (*Picea abies* (L.) Karst.) in the Babia Góra National Park, Poland. *Dendrochronologia* 16: 45-55.
- Bouriaud, O., J.-M. Leban, D. Bert and C. Deleuze. 2005. Intra-annual variations in climate influence growth and wood density of Norway spruce. *Tree Physiol.* 25:651-660.
- Briffa, K.R., F.H. Schweingruber, P.D. Jones, T.J. Osborn, S.G. Shiyatov and E.A. Vaganov. 1998. Reduced sensitivity of recent tree-growth to temperature at high northern latitudes. *Nature* 391: 678-681.
- Briffa, K.R., T.J. Osborn, F.H. Schweingruber, I.C. Harris, P.D. Jones, S.G. Shiyatov and E.A. Vaganov. 2001. Low-frequency temperature variations from a northern tree ring density network. *J. Geophys. Res.* 106:2929-2941.
- Briffa, K.R., T.J. Osborn, F.H. Schweingruber, P.D. Jones, S.G. Shiyatov and E.A. Vaganov. 2002. Tree-ring width and density around the Northern Hemisphere: Part 1, local and regional climate signals. *Holocene* 12:737-757.
- Büntgen, U., J. Esper, D.C. Frank, K. Nicolussi and M. Schmidhalter. 2005. A 1052-year tree-ring proxy of Alpine summer temperatures. *Clim. Dyn.* 25:141-153.
- Büntgen, U., D.C. Frank, M. Schmidhalter, B. Neuwirth, M. Seifert and J. Esper. 2006a. Growth/climate response shift in a long subalpine spruce chronology. *Trees* 20:99-110.
- Büntgen, U., D.C. Frank, R. Böhm and J. Esper. 2006b. Effect of uncertainty in instrumental data on reconstructed temperature amplitude in the European Alps. Ed. Heinrich, I. *Tree rings in archaeology, climatology and ecology, TRACE* 4:38-45.
- Büntgen, U., D.C. Frank, D. Nievergelt and J. Esper. 2006c. Summer temperature variations in the European Alps, AD 755-2004. *J. Climate* 19/21:5606-5623.
- Carrer, M., T. Anfodillo, C. Urbinati and V. Carraro. 1998. High altitude forest sensitivity to global warming: results from long-term and short-term analyses in the Eastern Italian Alps. *In Lecture notes in earth sciences: The impacts of climate variability on forests.* Vol. 74. Eds. M. Beniston and J.L. Innes. Springer-Verlag, Berlin, pp 171-189.
- Carrer, M. and C. Urbinati. 2004. Age-dependent tree-ring growth response to climate in *Larix decidua* and *Pinus cembra*. *Ecology* 85:730-740.
- Casty, C., D. Handorf and M. Sempf. 2005. Combined winter climate regimes over the North Atlantic/European sector 1766-2000. *Geophys. Res. Lett.* 32:doi:10.1029/2005GL022431.
- Chapin, F.S. and G.R. Shaver. 1996. Physiological and growth response of arctic plants to a field experiment simulating climatic change. *Ecology* 77:822-840.
- Cook, E.R. and K. Peters. 1981. The smoothing spline: A new approach to standardizing forest interior tree-ring width series for dendroclimatic studies. *Tree-Ring Bull.* 41:45-53.
- Cook, E.R. and K. Peters. 1997. Calculating unbiased tree-ring indices for the study of climatic and environmental change. *Holocene* 7:361-370.
- Cook, E.R., K.R. Briffa and P.D. Jones. 1994. Spatial regression methods in dendroclimatology: a review and comparison of two techniques. *Int. J. Climatol.* 14:379-402.
- Cook, E.R., K.R. Briffa, D.M. Meko, D.A. Graybill, and G. Funkhouser. 1995. The 'segment length curse' in long tree-ring chronology development for palaeoclimatic studies. *Holocene* 5:229-237.
- D'Arrigo, R.D., R.K. Kaufmann, N. Davi, G.C. Jacoby, C. Laskowski, R.B. Myneni and P. Cherubini. 2004. Thresholds of warming-induced growth decline at elevational tree line in Yukon Territory, Canada. *Global Biogeochem. Cycles* 18:doi:10.1029/2004GB002249.
- Desplanque, C., C. Rolland and F.H. Schweingruber. 1999. Influence of species and abiotic factors on extreme tree ring modulation. *Trees* 13:218-227.
- Durbin, J. and G.S. Watson. 1951. Testing for serial correlation in least squares regression. *Biometrika* 38:159-78.
- Eddy, J.A. 1976. The Maunder Minimum. *Science* 192:1189-1202.
- Eis, S., E.H. Garman and L.F. Ebell. 1965. Relation between cone production and diameter increment of Douglas-fir (*Pseudotsuga menziesii* (Mirb.) Franco), grand fir (*Abies grandis* (Dougl.) Lindl.) and western white pine (*Pinus monticola* Dougl.). *Can. J. Bot.* 43:1553-1559.
- Esper, J., E.R. Cook, P.J. Krusic, K. Peters and F.H. Schweingruber. 2003. Tests of the RCS method for preserving low-frequency variability in long tree-ring chronologies. *Tree-Ring Res.* 59:81-98.
- Esper, J., D.C. Frank, R.J.S. Wilson and K.R. Briffa. 2005a. Effect of scaling and regression on reconstructed temperature amplitude for the past millennium. *Geophys. Res. Lett.* 31:doi:10.1029/2004GL021236.
- Esper, J., R.J.S. Wilson, D.C. Frank, A. Moberg, H. Wanner and J. Luterbacher. 2005b. Climate: past ranges and future changes. *Sci. Rev.* 24:2164-2166.
- Feliksik, E. 1993. Teleconnection of the radial growth of fir (*Abies alba* Mill.) within central Europe. *Dendrochronologia* 11:171-175.
- Frank, D.C. and J. Esper. 2005a. Characterization and climate response patterns of a high elevation, multi species tree-ring network for the European Alps. *Dendrochronologia* 22:107-121.
- Frank, D.C. and J. Esper. 2005b. Temperature reconstructions and comparisons with instrumental data from a tree-ring network for the European Alps. *Int. J. Climatol.* 25:1437-1454.
- Fritts, H.C. 1976. *Tree rings and climate.* Academic Press, London, 567 p.
- Grudd, H., K.R. Briffa, W. Karlén, T.S. Bartholin, P.D. Jones and B. Kromer. 2002. A 7400-year tree-ring chronology in northern Swedish Lapland: natural climatic variability expressed on annual to millennial timescales. *Holocene* 12:657-665.
- Hegerl, G. C., T. J. Crowley, W. T. Hyde and D. J. Frame. 2006. Climate sensitivity constrained by temperature reconstructions over the past seven centuries. *Nature* 440:1029-1032.
- Helama, S., M. Lindholm, M. Timonen, J. Meriläinen and M. Eronen. 2002. The supra-long Scots pine tree-ring record for Finnish Lapland: Part 2, interannual to centennial variability in summer temperatures for 7500 years. *Holocene* 12:681-687.

- Hurrell, J. W., Y. Kushnir, G. Ottersen and M. Visbeck. 2003. An overview of the North Atlantic Oscillation. *Geophys. Mono.* 35 p.
- Jolly, W.M., M. Dobbertin, N.E. Ziermann and M. Reichstein. 2005. Divergent vegetation growth responses to the 2003 heat wave in the Swiss Alps. *Geophys. Res. Lett.* 32:doi:10.1029/2005GLO23252.
- Jones, P.D., K.R. Briffa and T.J. Osborn. 2003. Changes in the Northern Hemisphere annual cycle: implications for paleoclimatology? *J. Geophys. Res.* 108:doi:10.1029/2003JD003695.
- Kahle, H.P. 2006. Impact of the drought in 2003 on intra- and inter-annual stem radial growth of beech and spruce along an altitudinal gradient in the Black Forest, Germany. *In* *Tree Rings in Archaeology, Climatology and Ecology*. Ed. I. Heinrich. TRACE 4: 151–163.
- Kienast, F., O. Wildi and B. Brzeziecki. 1998. Potential impacts of climate change on species richness in mountain forests—an ecological risk assessment. *Biol. Conserv.* 83:291–305.
- Koncek M. 1974. *Klima Tatier*. Vyd. Slovenskoj Akad. Vied., Bratislava, 856 p.
- Körner, C. 1998. A re-assessment of high elevation treeline positions and their explanation. *Oecologia* 115:445–459.
- Kozłowski, T.T. and S.G. Pallardy. 1997. *Physiology of wood plants*. Academic Press, San Diego, 411 p.
- Leuzinger, S., G. Zotz, R. Asshoff and C. Körner. 2005. Response of deciduous forest trees to severe drought in Central Europe. *Tree Physiol.* 25:641–650.
- Luterbacher, J., D. Dietrich, E. Xoplaki, M. Grosjean and H. Wanner. 2004. European seasonal and annual temperature variability, trends and extremes since 1500 A.D. *Science* 303:1499–1503.
- Mäkinen, H., Nöjd, P. and P. Saranpää. 2003. Seasonal changes in stem radius and production of new tracheids in Norway spruce. *Tree Physiol.* 23:959–968.
- Mitchell, T.D. and P.D. Jones. 2005. An improved method of constructing a database of monthly climate observations and associated high-resolution grids. *Int. J. Climatol.* 25:693–712.
- Neuwirth, B., J. Esper, F.H. Schweingruber and M. Winiger. 2004. Site ecological differences to the climatic forcing of spruce pointer years from the Lötschental, Switzerland. *Dendrochronologia* 21: 69–78.
- Niedzwiedz, T. 1992. Climate of the Tatra Mountains. *Mt. Res. Dev.* 12:131–146.
- Oberhuber, W. 2004. Influence of climate on radial growth of *Pinus cembra* within the alpine timberline ecotone. *Tree Physiol.* 24: 291–301.
- Oleksyn, J., T. Modrzyński, M.G. Tjoelker, R. Zytowskiak, P.B. Reich and P. Karolewski. 1998. Growth and physiology of *Picea abies* populations from elevational transects: common garden evidence for altitudinal ecotypes and cold adaptation. *Funct. Ecol.* 12: 573–590.
- Osborn, T.J., K.R. Briffa and P.D. Jones. 1997. Adjusting variance for sample-size in tree-ring chronologies and other regional-mean time-series. *Dendrochronologia* 15:89–99.
- Peters, K., G.C. Jacoby and E.R. Cook. 1981. Principal component analysis of tree-ring sites. *Tree-Ring Bull.* 41:1–19.
- Raible, C.C., C. Casty, J. Luterbacher, A. Pauling, J. Esper, D.C. Frank, U. Büntgen, A.C. Roesch, P. Tschuck, M. Wild, P.L. Vidale, C. Schär and H. Wanner. 2006. Climate variability—observations, reconstructions, and model simulations for the Atlantic-European and Alpine region from 1500–2100 AD. *Clim. Change*. In press.
- Richman, M.B. 1986. Rotation of principal components. *J. Climatol.* 6:293–335.
- Rolland, C. 1993. Tree-ring and climate relationships for *Abies alba* in the internal Alps. *Tree-Ring Bull.* 53:1–11.
- Rolland, C., V. Petitcolas and R. Michalet. 1998. Changes in radial tree growth for *Picea abies*, *Larix decidua*, *Pinus cembra* and *Pinus uncinata* near the alpine timberline since 1750. *Trees* 13: 40–53.
- Rolland, C., C. Desplanque, R. Michalet and F.H. Schweingruber. 2000. Extreme tree rings in spruce (*Picea abies* (L.) Karst.) and fir (*Abies alba* Mill.) stands in relation to climate, site and space in the Southern French and Italian Alps. *Arct. Antarct. Alp. Res.* 32: 1–13.
- Saxe, H., M.G.R. Cannell, O. Johnsen, M.G. Ryan and G. Vourlitis. 2001. Tree and forest functioning in response to global warming. *New Phytol.* 149:369–399.
- Schär, C., P.L. Vidale, D. Lüthi, C. Frei, C. Häberli, M.A. Liniger and C. Appenzeller. 2004. The role of increasing temperature variability in European summer heatwaves. *Nature* 427:332–336.
- Schweingruber, F.H. 1996. *Tree rings and environment—dendrochronology*. Haupt, Bern, 609 p.
- Simkin, T. and L. Siebert. 1994. *Volcanoes of the world: A regional directory, gazetteer, and chronology of volcanism during the last 10,000 years*. 2nd Edn. Geoscience Press, Tucson, Arizona, 349 p.
- Sitch, S., B. Smith, I.C. Prentice, A. Arneeth, A. Bondeau, W. Cramer, J.O. Kaplan, S. Levis, W. Lucht, M.T. Sykes, K. Thonicke and S. Venevsky. 2003. Evaluation of ecosystem dynamic, plant geography and terrestrial carbon cycling in the LPJ dynamic global vegetation model. *Glob. Change Biol.* 9:161–185.
- Szychowska-Krapiec, E. 1998. Spruce chronology from Mt. Pilsko area (Zywiec Beskid Range) 1641–1995 AD. *Bull. Polish Acad. Sci., Earth Sci.* 46:75–86.
- Thuiller, W., S. Lavorel, M.B. Arujo, M.T. Sykes and I.C. Prentice. 2005. Climate change threats to plant diversity in Europe. *Proc. Natl. Acad. Sci. USA* 102:8245–8250.
- Tranquillini, W. 1964. The physiology of plants at high altitudes. *Annu. Rev. Plant Physiol.* 15:345–362.
- Trenberth, K. 1984. Some effects of finite sample size and persistence on meteorological statistics. Part I: Autocorrelations. *Mon. Weath. Rev.* 112:2359–2368.
- Vaganov, E. A., M.K. Hughes, A.V. Kirilyanov, F.H. Schweingruber and P.P. Silkin. 1999. Influence of snowfall and melt timing on tree growth in subarctic Eurasia. *Nature* 400:149–151.
- Wigley, T.M.L., K.R. Briffa and P.D. Jones. 1984. On the average of value of correlated time series, with applications in dendroclimatology and hydrometeorology. *J. Clim. Appl. Meteorol.* 23: 201–213.
- Wilson, R.J.S. and B.H. Luckman. 2003. Dendroclimatic reconstruction of maximum summer temperatures from upper tree-line sites in interior British Columbia. *Holocene* 13:853–863.